Journal of South American Earth Sciences 81 (2018) 153–164

Contents lists available at ScienceDirect

Journal of South American Earth Sciences

journal homepage: www.elsevier.com/locate/jsames

Geothermal potential assessment of the Nevado del Ruiz volcano based on rock thermal conductivity measurements and numerical modeling of heat transfer

Maria Isabel Vélez [a, *], Daniela Blessent [b], Sebastián Córdoba [b], Jacqueline López-Sánchez [b], Jasmin Raymond [a], Eduardo Parra-Palacio [b]

[a] Institut national de la recherche scientifique, Centre Eau Terre Environnement, Québec, Qc, Canada
[b] Universidad de Medellín, Programa de Ingeniería Ambiental, Medellín, Colombia

ARTICLE INFO

Article history:
Received 27 April 2017
Received in revised form
10 November 2017
Accepted 14 November 2017
Available online 15 November 2017

Keywords:
Nevado del Ruiz
Colombia
Geothermal potential
Thermal conductivity
OpenGeoSys

ABSTRACT

This work presents an estimation of the geothermal potential of the Nevado del Ruiz (NDR) volcano, bridging the knowledge gap to develop geothermal energy in Colombia and improve resource estimates in South America. Field work, laboratory measurements, geological interpretations, 2D numerical modeling, and uncertainty analysis were conducted to the northwest of the NDR to assess temperature at depth and define thermal energy content. About 60 rock samples were collected at outcrops to measure thermal conductivity with a needle probe. A 2D numerical model, built from an inferred geological cross-section, was developed with the software OpenGeoSys to simulate the underground temperature distribution and then estimate the geothermal potential of a 1 km^2 area with sufficient temperature, assuming a recovery factor equal to 2.4% and a 30 years exploitation time. Coupled groundwater flow and heat transfer were simulated in steady-state considering two different thermal conductivity scenarios. Results show that the average estimated potential is 1.5×10^{-2} MW_t m^{-1} of the reservoir thickness, considering temperatures greater than 150 °C located at a depth of approximately 2 km, in a selected area situated outside of the Los Nevados National Natural Park (NNP), to avoid any direct intervention on this protected area. According to a Monte Carlo analysis considering pessimist and optimist scenarios of thermal conductivity, the estimated geothermal power was 1.54×10^{-2} MW m^{-1} ($\sigma = 2.91 \times 10^{-3}$ MW m^{-1}) and 1.88×10^{-2} MW/m ($\sigma = 2.91 \times 10^{-3}$ MW m^{-1}) for the two modeling scenario considered.

1. Introduction

Estimation of the worldwide geothermal potential is a challenging task, with pitfalls due to uncertainties and knowledge gaps (Bertani, 2009). This worldwide potential is usually determined by adding up the estimates for individual countries or regions, but the task is difficult, since the geothermal energy potential is unknown in many countries (Stefánsson, 1998, 2005; Fridleifsson, 2003). This lack of information is particularly important for developing countries of Latin America such as Colombia, where field data are sparse, if not non-existent. In the recent report published by Bertani (2016), Colombia is indicated as a country where there is no geothermal development yet and no additional information is provided. This situation is not unique to Colombia but common to South America where untapped geothermal resources still need to be defined. Recent studies on the estimation of the geothermal potential have been conducted in few countries of South America, where there are no operating geothermal power plants. Aravena et al. (2016) estimated the geothermal potential of high enthalpy geothermal areas of Chile to 659 MWe, applying numerical methods and including inferred resources. Invernizzi et al. (2014) described a preliminary assessment of the geothermal potential of Rosario de la Frontera area to the northwest of Argentina, indicating 5.6×10^{18} J of heat stored in the rock and 0.8×10^{18} J in the geothermal fluids. Ongoing exploration has taken place in Bolivia at the Laguna Colorado Field, while an estimation of 150 MWe has been indicated for two geothermal fields in Peru (Bertani, 2016).

Such geothermal resource assessment depends on a variety of aspects that can be grouped as follows: geological, physical, technological, and economical (Muffler and Cataldi, 1978). The choice of

* Corresponding author.
E-mail address: Maria_Isabel.Velez_Marquez@ete.inrs.ca (M.I. Vélez).

https://doi.org/10.1016/j.jsames.2017.11.011
0895-9811/

a method for reservoir assessment depends on the available data, the purposes of the assessment and the accuracy needed (Barylo, 2000). Muffler and Cataldi (1978) grouped the methods for geothermal resource assessment in four categories: 1) surface heat flux method, 2) volume method, 3) planar fracture method, and 4) magmatic budget method. The volumetric method is commonly used for geothermal potential estimation at the early stage of geothermal resource assessment. This method can be used when there are no or not enough exploratory wells nor permeability data and is thus a preferred option for early stage assessment. A recovery factor is considered by the volumetric method to calculate the static heat reserve in the reservoir and estimates the extractable energy (Barylo, 2000). Stochastic simulations and risk analysis are frequently used in conjunction with the volume method to estimate the range and the probable distribution of stored heat reserves and exploitable energy. These analyses have been borrowed from the oil industry, where they have been used for a long time to estimate probabilistic hydrocarbon-in-place and oil and gas reserves in sedimentary basins (Ofwona, 2008). Such stochastic simulations, commonly based on the Monte Carlo method, are particularly beneficial where data is scanty and uncertainties high (Ofwona, 2008).

This work is an attempt to bridge the knowledge gap in Colombia and South America by describing the geothermal potential assessment of an area of the Nevado del Ruiz (NDR) volcano located in the Colombian Central Cordillera. Similar geological settings can be expected for geothermal fields of the Colombian Central Cordillera, where the described method could be applied. The geothermal resource assessment of the NDR volcano was actually based on 1) thermal conductivity laboratory measurements on rock samples collected at outcrops, 2) an inferred geological cross-section, 3) coupled groundwater flow and heat transfer numerical modeling with the OpenGeoSys software (Böttcher et al., 2016), 4) volumetric resource estimation method, and 5) uncertainty analysis conducted with the @RISK software (Ofwona, 2008; Walsh, 2013; Yang et al., 2015). The NDR volcano is the best known geothermal area of Colombia, where the interest of several entities converge (Alfaro, 2015). However, geothermal development in Colombia is incipient in comparison with other Latin America countries with similar volcanic environments (Bertani, 2016). This case study of the NDR area contributes to fill this lack of information and to help develop the geothermal potential in Colombia.

2. Geological settings

Volcanism in the Colombian Central Cordillera is defined by a complex tectonic framework, since the country is located at the intersection of South America, Nazca, and Caribbean tectonic plates. The subduction of the Nazca below the South American Plate is the governing mechanism triggering volcanic activity due to the rapid convergence of 58 mm/year occurring at the Colombia-Ecuador trench (Trenkamp et al., 2002). The NDR is an active stratovolcano enclosing the Los Nevados National Natural Park (NNP) covering an area of approximately 58300 ha in the middle of the Colombian Central Cordillera (4° 53′43 “N, 75° 19′21” W), between the limits of Caldas and Tolima departments of Colombia (Fig. 1).

The NDR is part of the volcanic complex Ruiz-Tolima and contains three craters: the Olleta, the Piraña, and the Arenas. The Arenas crater has been the source of the most recent activity: an explosive eruption occurred in November 1985 (Naranjo et al., 1986), while variations in the volcanic activity and ash emissions have been registered since October 2010 until these days.[1] Based on seismicity, geochemistry and geology of the volcano, Londoño and Sudo (2002) presented a conceptual model of its activity, identifying three heat sources located at different depths: the first one from 2 to 3 km, the second one from 5 to 10 km, and the deepest zone from 10 to 15 km. Stix et al. (2003) presented a conceptual view of magma ascent through a plexus of cracks in the crust, from the source main reservoir located at depth comprised between 9 and 15 km.

The geological situation of the Ruiz region is featured by several Tertiary and Quaternary volcanic edifices and by a number of thermal springs. The reconstruction of the stratigraphic sequences is difficult because the oldest metamorphic and sedimentary rocks located at the base of the volcanic complex are often crossed or covered by igneous rocks that obliterate contacts (Arango et al., 1970). Among all geological units described by González (2001), those that are identified in the inferred geological cross-section described later, are the Cajamarca metamorphic complex (Pes), the Quebradagrande Complex (Kvc and Ksc), the Andesite unit (NgQa), pyroclastic rocks (Qto), glacial deposits (Qg), volcanic mud flows or lahars (Qfl), and recent alluvial deposits (Qar). The Cajamarca metamorphic complex, which makes up the regional basement of the Colombian Andes, encloses a wide range of lithological types. The pelitic complex (Pes) includes phyllites, sericite, and mica schists. There is evidence that this complex has undergone a greenschists facies metamorphism, while, locally, some rocks belonging to the amphibolites facies can be observed. The Quebradagrande Complex is composed of sedimentary rocks (Ksc), such as black shales, sandstones, conglomerates, limestones, with dynamic metamorphism and occasionally fossils. Volcanic rocks (Kvc), such as basalts, pyroclastic flows and diabasic dykes, have undergone prehnite-pumpellyite facies metamorphism. The Andesite unit (NgQa) has a composition ranging from andesitic to dacitic, and basaltic at fewer locations. The andesitic flows are macroscopically homogenous and have a porphyritic texture. The lahars or volcanic mud flows (Qfl) include blocks of andesitic-dacitic lava with variable diameter from few centimeters to more than 5 m. The pyroclastic rocks (Qto) may reach a thickness of 30 m. The recent alluvial deposits (Qar) cover older rocks close to rivers and creeks and have a variable thickness, which is generally less than 20 m. The glacial deposits (Qg) are associated to the Pleistocene glaciations that covered the Colombian Central Cordillera above 3000 m a.s.l.

3. Previous studies on the Nevado del Ruiz geothermal resources

The first geothermal study on the Nevado del Ruiz site was conducted towards the end of the 1960s by the Italian company ENEL (Ente Nazionale per la Energia Elettrica) in collaboration with the CHEC (Central Hidroeléctrica de Caldas) and described lithostratigraphic features, volcanology, structural events and hydrogeology of the NDR complex (Arango et al., 1970). Based on isotopic analysis, Arango et al. (1970) proposed a first tentative hypothesis of a shallow hydrothermal system clearly separated from a deep regional system. They identified the presence of a thick caprock, formed by the upper part of the metamorphic complex and separating the two major circulation-systems to the west, northwest and north of the Ruiz edifice. CHEC subsequently published a technical report describing the geological context of the NDR with details about the volcanology, geochemistry and geophysical characteristics of the area (CHEC et al., 1983). Two years after, the NDR volcano erupted during November 1985 (Melson et al., 1990; Thouret, 1990; Vatin-Pérignon et al., 1990), causing the Armero

[1] http://www2.sgc.gov.co/Manizales.aspx.

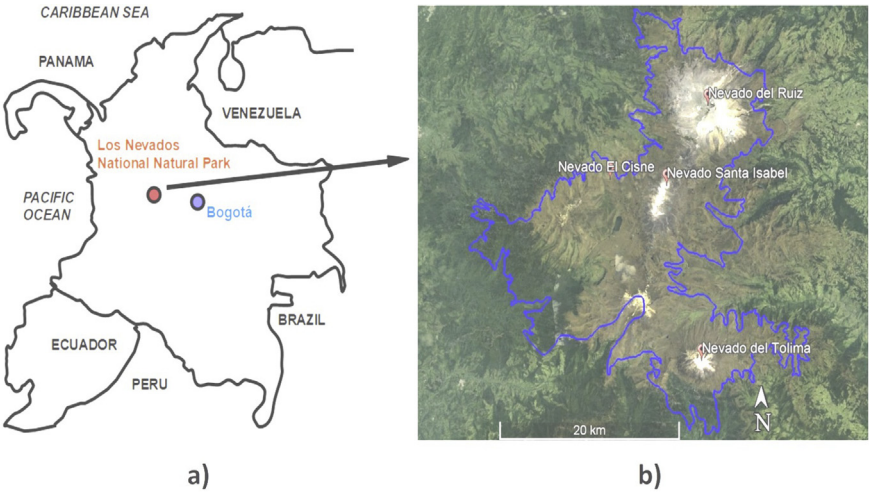

Fig. 1. a) Location of the Los Nevados NNP in Colombia and b) its neighboring Colombian departments (Risaralda, Caldas, Tolima, Quindío) and the main volcanoes (modified from Parques Nacionales Naturales de Colombia, 2007).

tragedy with about 25 000 casualties and leaving aside the geothermal explorations.

Field work restarted only in 1997 when the only deep geothermal exploration well in Colombia (Las Nereidas well) was drilled to a depth of 1466 m on the western side of the NDR, at 3450 m a.s.l. In this borehole, seven lithological units with hydrothermal alteration were identified. The measured bottom hole temperature was about 200 °C (Monsalve et al., 1998). Recent studies were conducted from 2011 to 2013: Rayo-Rocha and Zuluaga (2011) indicated, through petrographic and geochemical analysis of lava samples, the existence of a deep magmatic chamber feeding a shallower chamber. Rojas (2012) presented the temperature profiles measured in three 300 m deep wells that were drilled in 2011 with the objective to measure the geothermal gradient. Forero (2012) provided a characterization of hydrothermal alteration to the northwest of the volcano that led to a simple conceptual model of the geothermal reservoir. Almaguer (2013) presented the results from a magnetotelluric study conducted to the North of the volcano, where high electrical conductivity areas confined by sections of moderated resistivity were interpreted as a possible reservoir and caprock, respectively. After this renewed interested, the Colombian ISAGEN company then applied for an environmental license following the realization of the environmental impact study to drill the first of five planned exploratory wells on the western flank of the NDR volcano (Alfaro, 2015). González-Garcia and Jessell (2016) published a first 3D geological model for the Ruiz-Tolima volcanic massif, using the Monte Carlo method to characterize geological uncertainty. Their model represents the probability of occurrence of geological units, suggesting where future exploratory work should be conducted.

4. Material and methods

4.1. Rock sampling and geological cross-section

Field work was conducted in November 2014 over two itineraries with an approximate length of 26 km (Villamaria and Enea route) outside of the Los Nevados NNP (Fig. 2). The objective of rock sampling was to collect the main lithologies characterizing the study area. Three rock samples were collected at each sampling locations (Table 1). The geological cross-section AA' (Fig. 2) starts from the NDR peak (A') and goes up to the outcrops of the Quebradagrande Complex (Ksc and Kvc), located on the northwest of the NDR peak. The cross-section is drawn close to the sampling points and hot springs located along the Villamaria route and crosses the Cajamarca Complex (Pes), which is one of the lithologies of most interest, because this metamorphic complex might be part of a potential geothermal reservoir (Almaguer, 2013), together with the Quebradagrande Complex (CHEC, 1983). Although this hydrothermal system has been studied since the seventies, the location of a porous reservoir is not publicly known, but it is suggested that faults provide structural control of the hydrothermal flow (González-Garcia et al., 2015). Geological observations indicate that the primary porosity of potential reservoir units is low and the potential to find natural hydrothermal systems is related to secondary porosity. However, faults were not considered in this work since the objective is to provide a quantitative methodology to estimate the geothermal resource potential based on heat stored in the basement rock. Fault zones shall be considered in further studies as structural geology information becomes available together with 3D geological models to provide a more accurate estimation of this geothermal potential.

4.2. Thermal conductivity measurements

Thermal conductivity measurements were made at the Institut national de la recherche scientifique Centre Eau Terre Environnement (INRS-ETE) in Québec City (Canada), following the ASTM methodology (ASTM, 2008). Thermal conductivity was measured inserting the KD2 Pro transient needle probe RK- 1 (Decagon Devices Inc., 2008) in a 3.9 mm diameter hole previously drilled in each rock sample that has been previously saturated when having visible porosity. The hole, approximately 6 cm deep, was drilled with a rotary hammer in the middle of a flat side of each rock sample, to ensure uniform heat transfer in every direction in the sample during the measurement. The space between the needle and the hole was filled with thermal grease to ensure thermal contact. The heating needle had a temperature sensor. Heat was injected through the needle for 5 min, while temperature was monitored, and a 5 min recovery period was considered after the heating pulse. The thermal conductivity was determined from the analysis of the temperature increment ΔT, which depends on the distance r from the source and on the time t, according to the infinite line source equation (Carslaw and Jaeger, 1947):

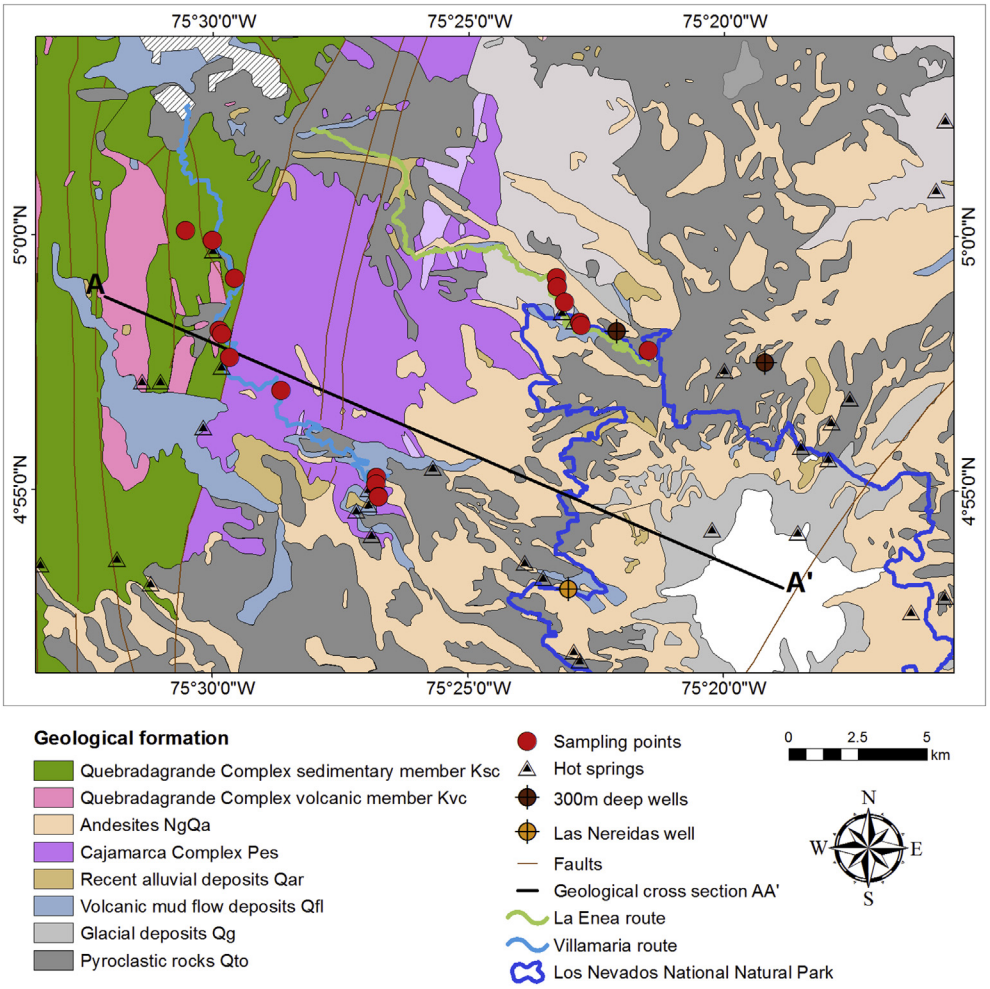

Fig. 2. Geological map of the study area showing the sampled outcrops. Simplified from INGEOMINAS geological maps sheet Nos. 206 and 225 (Mosquera et al., 1998a, 1998b).

Table 1
Sampling points coordinates and mesoscopic characterization.

Sample #	Code	X coordinate[a]	Y coordinate[a]	Lithologic unit	Rock type
1	2014 MI 1	4.998	−75.500	Quebradagrande Complex	Sandstone
2	2014 MI 2	5.002	−75.509	Quebradagrande Complex	Sandstone
3	2014 MI 3	4.986	−75.493	Quebradagrande Complex	Sandstone
4	2014 MI 4	4.969	−75.498	Quebradagrande Complex	Schist
5	2014 MI 5	4.968	−75.497	Quebradagrande Complex	Schist
6	2014 MI 6	4.968	−75.497	Cajamarca Complex	Quartz phyllite
7	2014 MI 7	4.960	−75.495	Cajamarca Complex	Schist
8	2014 MI 8	4.986	−75.388	Andesite unit	Andesitic lava flows
9	2014 MI 12	4.972	−75.380	Andesite unit	Andesite
10	2014 MI 13	4.972	−75.380	Andesite unit	Andesite
11	2014 MI 14	4.972	−75.380	Volcanic mud flow	Volcanic mud flows deposits
12	2014 MI 15	4.971	−75.380	Volcanic mud flow	Volcanic mud flows deposits
13	2014 MI 16	4.963	−75.358	Andesite unit	Andesite
14	2014 MI 17	4.949	−75.478	Cajamarca Complex	Quartz phyllite
15	2014 MI 18	4.921	−75.446	Andesite unit	Andesite
16	2014 MI 19	4.919	−75.447	Andesite unit	Andesite
17	2014 MI 20	4.915	−75.446	Cajamarca Complex	Schist
18	2014 MI 21	4.915	−75.446	Cajamarca Complex	Schist

[a] WGS84 coordinate system.

$$\Delta T(r,t) = \frac{-q}{4\pi\lambda} E_i\left(\frac{-r^2}{4\alpha t}\right) \quad (1)$$

where q (W m^{-1}) is the heat input per unit length, α (m^2 s^{-1}) is the thermal diffusivity, r (m) is the needle radius, E_i is the exponential integral that can be developed as a Taylor series, λ (W m^{-1} K^{-1}) is the thermal conductivity of the rock sample, and t (s) is the time. From Eq. (1), the temperature can be approximated to a linear

equation in a semi-logarithmic plot, where the slope is related to the thermal conductivity λ:

$$T(t) \approx \frac{q}{4\pi\lambda} \ln(t) + C \quad (2)$$

Thermal conductivity measurements were performed automatically at time intervals of 1 h to ensure that temperature returned to the equilibrium before doing a new measurement. Before and after each measurement, calibration was required to determine the correction factor *CF* Eq. (3), which compares the thermal conductivity of a known material ($\lambda_{material}$), a standard plastic cylinder supplied with the KD2 Pro thermal properties analyzer, with the one obtained experimentally ($\lambda_{measured}$), to adjust the measured thermal conductivity (ASTM, 2008):

$$CF = \frac{\lambda_{material}}{\lambda_{measured}} \quad (3)$$

4.3. Heat capacity estimation

Heat capacity was estimated according to the mesoscopic characterization of each rock sample based on the values provided by Waples and Waples (2004). Although approximate, this estimation is suitable since heat capacity does not show large variation within different rock types. The great majority of the specific heat capacities of minerals at ±20 °C is between 600 and 900 (J kg^{-1} K^{-1}), with a strong preference for values between 800 and 900 (J kg^{-1} K^{-1}).

4.4. Numerical modeling

To provide an estimation of the geothermal potential for the study area, numerical modeling was performed, since analytical methods can difficultly cope with irregular topography. It has long been recognized that topography affects heat flow and topographic correction has been based on identification of valleys and hills (Westaway and Younger, 2013). Nevertheless, the topography of the geological cross-section AA' has a saw-tooth like profile (Fig. 3) rather than a valley or a hill. Therefore, numerical modeling allowed considering almost the real topography in the simulated domain. The software OpenGeoSys (OGS), a scientific open-source initiative for numerical simulation of thermo-hydro-mechanical/chemical processes in porous and fractured media (Böttcher et al., 2016), was used to build a numerical model to estimate underground temperature and quantify geothermal resources. The GMSH mesh generator (Geuzaine and Remacle, 2009) and the Tecplot software were used to build the mesh and to visualize the numerical results, respectively. Fully saturated steady-state groundwater flow and heat transfer were the physical processes considered. Governing equations and specifications for modeling of geothermal processes were presented in detail by Böttcher et al. (2016) and therefore are not repeated here.

4.5. Geothermal resources evaluation

The quantification of geothermal resources was achieved for an area characterized by a temperature greater than 150 °C located outside of the Los Nevados NNP, at a depth between 2 and 3 km, and at a distance of 14–15 km from the left-hand side of the geological cross-section AA' (Fig. 3). An area of 1 km^2 was considered for the estimation of the geothermal potential, since the reservoir spatial delimitation is currently uncertain and needs further field investigations, such as geophysical surveys, to better identify permeable formations. Both temperature (150 °C) and depth (3 km) are the recommended values based on economic feasibility of geothermal exploration in Colombia (Bernal et al., 2000). The temperature of 150 °C can also be used to define high enthalpy systems according to Lee (1996).

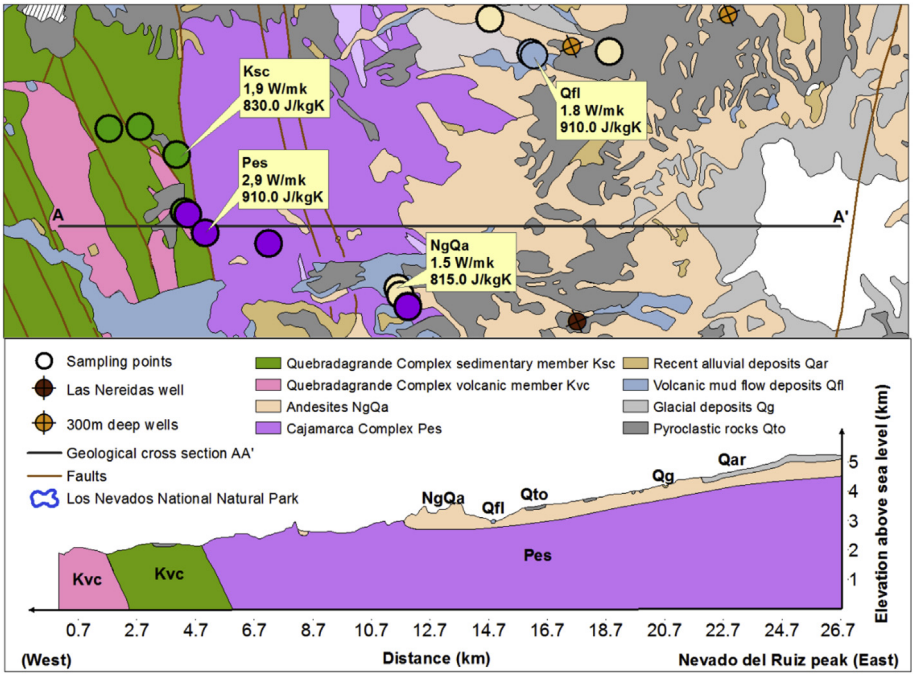

Fig. 3. Inferred geological cross-section AA′ and thermal properties evaluated for lithological units Pes, NgQa, Qfl, Ksc. Geological map simplified from INGEOMINAS geological maps sheet Nos. 206 and 225 (Mosquera et al., 1998a, 1998b).

Subsurface heat stored was evaluated in the zone of interest (Fig. 3) with the following equation:

$$Q_r = \rho \cdot C \cdot A \cdot (T_d - T_0) \quad (4)$$

where Q_r (J m^{-1}) is the available subsurface heat per unit width of the reservoir, ρ (Kg m^{-3}) is the rock density, C (J Kg^{-1} K^{-1}) is the rock heat capacity, A (m^2) is the area surrounding each selected point in the zone of interest, T_d (K) is the temperature at depth in the zone of interest and T_0 (K) is the temperature at the surface. Eq. (5) gives the total accumulated heat stored in the subsurface, but only a part of this quantity can be actually extracted. Therefore, the geothermal potential was estimated considering a recovery factor R, which is related to the available and exploitable energy (Calcagno et al., 2014) and depends on the porosity and on the permeability of the lithological formations of the geothermal reservoir (Walsh, 2013). The geothermal potential P_G (W) was finally calculated considering resource exploitation for a time t equals to 30 years:

$$P_G = R \cdot \frac{Q_r}{t} \quad (5)$$

In this case study, the geothermal potential was calculated using a recovery factor $R = 2.4\%$, which was reported by Calcagno et al. (2014) as the minimum recovery factor for fractured aquifers, as the potential NDR reservoir is hosted in low permeability basement rocks crossed by regional faults. Faults are expected to have an impact on the circulation of hydrothermal fluids in the NDR geothermal reservoir (Mejía et al., 2012). Further studies will consider the effect of faults, which do not cross the zone of interest selected in this work based on outcrops visited during field work. Conductive and advective heat transfer through the low-permeability rock matrix are the main processes considered in this study to provide a first estimate of the heat content in order to calculate geothermal resources.

Uncertainty analysis was conducted with Monte Carlo simulations using the @RISK software. The variables considered for uncertainty analysis were the temperature at depth T_d and the recovery factor R. T_d depends on the thermal conductivity and on the heat flow according to steady-state heat transfer that is conduction dominated in the numerical model.

5. Results

5.1. Laboratory measurements

The lithologic units identified at the 18 sampling locations (Table 1) were the Quebradagrande sedimentary Complex (Ksc), the Cajamarca Complex (Pes), the Andesite unit (NgQa) and the volcanic mud flow or lahars (Qfl). The Quebradagrande volcanic complex (Kvc) was not collected in the field since the access route did not lead to its outcrop (Fig. 2).

The thermal conductivity and the specific heat capacity (Table 2) associated to each lithology were calculated as the mean of the values obtained for all the samples belonging to the same unit, except for the thermal conductivity of the Andesite (NgQa). The thermal conductivity of sample 2014 MI 16 was higher than the other samples taken at the same location and the mean would be significantly affected by this extreme value. Then, the median was used because it was considered to better represent the thermal conductivity of this lithologic unit. Sample 5 of the Quebradagrande Complex (λ = 4.26 W m^{-1} K^{-1}) was further excluded from the determination of the mean thermal conductivity because it was taken in a fault zone that did not represent the general characteristics of this geological complex.

The thermal conductivity values obtained for the Quebradagrande Complex and volcanic mudslides did not show significant variation since most of the values were close to 2.0 W m^{-1} K^{-1}. The Andesite unit showed the lowest thermal conductivity value (1.2 W m^{-1} K^{-1}), while the Cajamarca Complex showed the highest value (2.9 W m^{-1} K^{-1}). Inferred heat capacity ranges from 815 to 1140 J kg^{-1} K^{-1}.

5.2. Geological cross-section

The thickness of the lithologic units in the geological cross-section AA' was based on a previous cross-section of the NDR volcano published by Central Hidroelectrica de Caldas (CHEC et al., 1983). Outcrops of the Quebradagrande and Cajamarca complexes are shown on this inferred geological cross-section (Fig. 3). The Andesite unit is approximately 500 m thick (CHEC et al., 1983) and lies above the Cajamarca Complex. It is possible to see the different superficial deposits (Qto, Qar, Qg, Qfl) produced by the volcanic activity during the Quaternary period. The two members of the Quebradagrande Complex (Ksc y Kvc) are located on the west end

Table 2
Measured thermal conductivity λ and heat capacity C estimated from Waples and Waples (2004).

Lithologic unit	Sample code	Rock sample λ (W m^{-1} K^{-1})	Mean λ (W m^{-1} K^{-1})	Rock sample C (J kg^{-1} K^{-1})	Mean C (J kg^{-1} K^{-1})
Quebradagrande Complex sedimentary member (Ksc)	2014 MI 1	1.98	1.92	775	830
	2014 MI 2	1.15		775	
	2014 MI 3	2.63		910	
	2014 MI 5	4.26		860	
Andesite (NgQa)	2014 MI 8	1.34	1.23[a]	815	815
	2014 MI 12	1.33			
	2014 MI 13	0.91			
	2014 MI 16	3.29			
	2014 MI 18	1.12			
	2014 MI 19	1.08			
Volcanic mud flow deposits (Qfl)	2014 MI 14	1.59	1.89	840	840
	2014 MI 15	2.18			
Cajamarca Complex (Pes)	2014 MI 6	3.18	2.98	1090	910
	2014 MI 7	2.89		790	
	2014 MI 17	2.75		1090	
	2014 MI 20	2.87		790	
	2014 MI 21	3.22		790	

[a] Thermal conductivity of the andesite unit was calculated as the median of the sample values.

of the cross-section and are dipping to the East.

5.3. Underground temperature model

The simulated domain was based on the inferred geological cross-section AA' (Fig. 3), where superficial geological deposits (Qar, Qfl, Qg, and Qto) were neglected, since their thickness was small enough to have a negligible influence on the underground temperature (Fig. 4) due to their limited spatial extent. The zone of interest to quantify geothermal resources was delimited considering temperatures >150 °C and depth <3 km, although groundwater flow and heat transfer was simulated over the whole cross section.

The triangular mesh built with GMSH has 4179 elements, which were refined close to the top of the domain to properly capture the topographic variations. Groundwater flow boundary conditions were hydraulic heads equal to the topographic elevation at the lateral extremities of the model, while the top and bottom boundaries were considered impermeable (Fig. 4). The top heat transfer boundary was a constant temperature determined from an elevation-dependent temperature profile, varying from +18 to −5 °C (CORPOCALDAS, 2007). Adiabatic conditions were set to the left and right of the domain. The bottom heat transfer boundary condition was a linearly variable heat flux defined considering the maximum, the minimum, and the mean heat flow values of the area. The minimum value, 0.12 W m^{-2}, was equal to the smallest heat flow in the study area, according to the Colombian heat flow map (INGEOMINAS, 2000); the mean value, 0.178 W m^{-2}, was evaluated from the geothermal gradient measured in the 300 m deep wells presented by Rojas (2012); the maximum value, 0.366 W m^{-2}, was estimated from the temperature gradient observed at the Nereidas well (Bernal et al., 2000).

An internal heat source was added to take into account the heat generation by the decay of radioactive elements. Concentrations of uranium, thorium and potassium for the average continental crust were considered (Turcotte and Schubert, 2014). The internal heat production was calculated as (Bucker and Rybach, 1996):

$$A = 10^{-5} \cdot \rho \cdot (9.52[U] + 2.56[Th] + 3.48[K]) \quad (6)$$

where A (μW m^{-3}) is the internal heat production, ρ (kg m^{-3}) is the average rock density, [U] (ppm) is the concentration of uranium, [Th] (ppm) is the concentration of thorium, [K] (%) is the concentration of potassium. The value calculated for the average continental crust was 0.866 μW m^{-3}, which was comprised within the range of common values for this parameter (Bédard et al., 2016).

A sensitivity analysis was conducted to define proper values for domain depth and mesh size. The domain depth has an impact because the heat transfer under the simulated conditions is dominantly vertical and affected by the irregular topography. For example, if the depth is lower, the heat source is closer to the surface, affecting the simulated temperature and the final geothermal potential estimation. The domain depth was defined on the right-hand side of the cross-section, where is located the NDR peak (Fig. 3). Depths of 3, 5, 7, 10, 12, 14, and 18 km were considered in the sensitivity analysis. Mesh resolution was varied from 200 m to 600 m; since mesh is always automatically refined close to the topography, these resolutions represent the average element size. The criterion to choose the appropriate values was based on the variation of the simulated temperature between two successive simulation results with varying depth or mesh resolution. The final depth and mesh resolution were chosen when the minimum temperature variation was observed between simulations. The selected model was 7 km deep and had an average mesh element size of 400 m.

The thermal properties of the main geological units inferred from the field characterization and hydraulic properties estimated according to Freeze and Cherry (1979) were used as inputs for the numerical simulations (Table 3). Since samples were not available for the Kvc volcanic complex, values equal to those of Ksc were assumed. The Kvc formation is, however, located on the left-hand side of the geological cross-section and was believed to have a small effect on the simulated temperature in the area of interest, which is located approximately 14 km away (Fig. 4). This was in fact verified by additional simulations whose results are not presented here.

Two modeling scenarios were considered (Table 4) to compare a case characterized by constant thermal conductivity in the Cajamarca Complex Pes (Case A), with another case characterized by a temperature dependent thermal conductivity (Case B). Three sublayers were defined in the Cajamarca Complex for Case B (Fig. 5), based on the temperature dependent thermal conductivity calculated with the relation proposed by Clauser (2014):

$$\lambda = A + \frac{B}{350 + T} \quad 0°C \le T \le 800°C \quad (7)$$

where A (W $m^{-1}K^{-1}$) = 0.75 and B (W m^{-1}) = 705 for metamorphic rocks.

Eq. (7) was applied to the simulated temperatures from Case A to define three regions with different thermal conductivity in the metamorphic Cajamarca Complex, since a temperature dependent thermal conductivity was not available in OpenGeoSys. This approach allowed investigating the effect of temperature on thermal conductivity, although it is approximate.

The maximum temperature simulated for Case A was 532 °C at the bottom right-hand side of the profile, where the largest heat flux (0.366 W m^{-2}) was applied as a bottom boundary condition (Fig. 6a). The temperature was greater than 150 °C in the area of

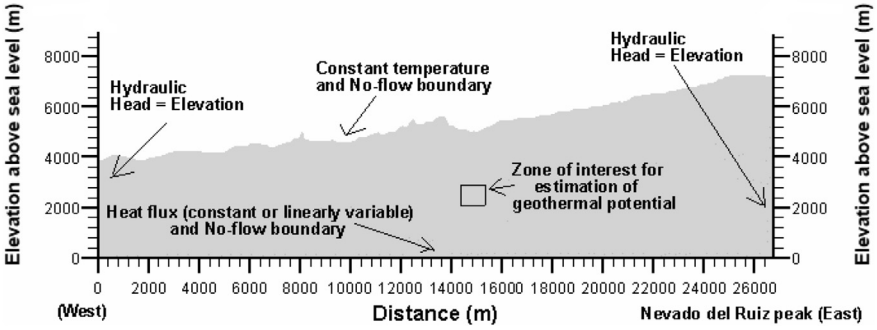

Fig. 4. Model extension, boundary conditions, and selected zone of interest (1 km^2) for the estimation of the geothermal potential.

Table 3
Properties of material used for numerical simulations.

	Pes	NgQa	Kvc	Ksc
Saturated hydraulic conductivity K (m s^{-1})	1.0×10^{-11}	1×10^{-9}	1×10^{-10}	1×10^{-10}
Porosity n (–)	0.05	0.15	0.05	0.05
Thermal conductivity Case A (W m^{-1} K^{-1})	2.98	1.22	1.92	1.92
Thermal conductivity Case B (W m^{-1} K^{-1}) (see Fig. 5)	Layer 1:2.66 Layer 2:2.09 Layer 3:1.81	1.22	1.92	1.92
Specific heat capacity (J kg^{-1} K^{-1})	910	815	830	830
Density (kg m^{-3})	2700	2650	2700	2700

Table 4
Modeling scenarios considered.

Scenario	Description
Case A	Constant thermal conductivity for the Cajamarca Complex (Pes)
Case B	Temperature dependent thermal conductivity for the Cajamarca Complex (Pes)

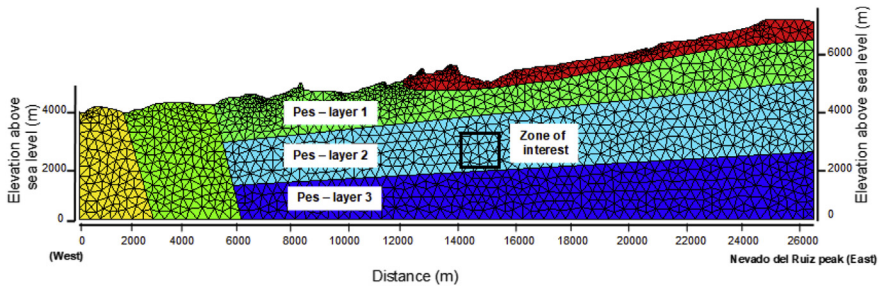

Fig. 5. Triangular mesh and sub-layers 1, 2, and 3 in the Cajamarca metamorphic complex (Pes) close to the zone of interest, for simulation scenario Case B.

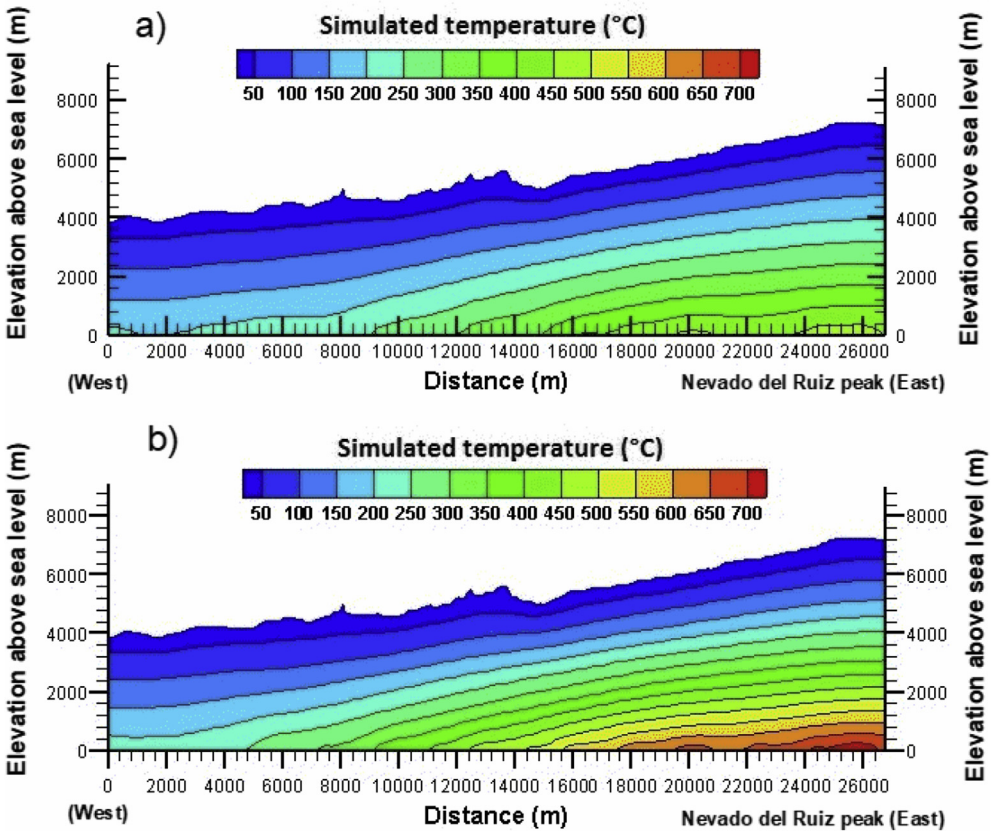

Fig. 6. Simulated temperature distribution for a) Case A and b) Case B.

interest at a distance of 14–15 km and at a depth of 2–3 km, indicating that high-enthalpy geothermal resources (Lee, 1996) are located outside of the Los Nevados NNP, where they may be exploited.

The maximum simulated temperature increased in Case B (Fig. 6b), with a temperature dependent thermal conductivity in the Cajamarca Complex (Pes). This temperature increase was due to the lower thermal conductivity providing insulation in the deeper region of the cross-section. The maximum simulated temperature was now 753 °C, while it was 532 °C in Case A. Nevertheless, the increase in temperature was somewhat more moderate in the area of interest, with an average increase of 45 °C. Simulated temperatures were now greater than 200 °C in almost all the area of interest. This scenario was considered as more realistic, since it takes into account the decreasing thermal conductivity with temperature, although still approximate.

The influence of the internal heat production due to the radioactive decay appeared not be significant since a small value of internal heat generation was calculated (0.866 $\mu W\ m^{-3}$), compared to the heat flux applied to the bottom boundary (mean value of 0.2 $W\ m^{-3}$).

5.4. Geothermal resource evaluation

In order to quantify the influence of the temperature at depth T_d and the recovery factor R on the geothermal resources evaluation, Case A and Case B were considered. The simulated temperatures in the area of interest for simulation scenarios Case A and Case B are shown in Fig. 7, where the triangular mesh is also illustrated. Using Eq. (4), the available subsurface heat Q_R was estimated, exporting the simulated temperature at points uniformly distributed over the area of interest along five 1000 m high vertical segments (from a depth of 2000 m–3000 m) located 200 m apart. Since each segment had 10 points along its height, the area A associated with each point is 22 000 m^2 (200 m × 110 m): the density and heat capacity of the Cajamarca Complex (Table 3) were considered to calculate with Eq. (5) the geothermal potential P_G for a 30 y exploitation period with R = 2.4% as recovery factor (Table 5). The geothermal potential was larger for Case B, since higher temperatures were obtained using a temperature dependent thermal conductivity, for the same heat flux bottom boundary condition. Nevertheless, geothermal power resources for both cases were on the same order of magnitude (1.36×10^{-2} and $1.67 \times 10^{-2}\ MW_t\ m^{-1}$).

5.5. Uncertainty analysis

Uncertainty analysis of the geothermal potential was conducted for the area of interest (Fig. 4), using the temperature variation ΔT and the recovery factor R as input variables with 10000 Monte Carlo iterations. Uniform distributions were used to define the variation of the parameters. Recovery factor varied from 2.4% to 3% and the temperature variation from 160.5 °C to 235 °C.

The temperature intervals between 156 °C and 239 °C and between 183 °C and 301 °C were obtained for the two scenarios, Case A and Case B, respectively. The mean thermal energy for Case A, considering homogenous thermal conductivity in the Cajamarca Complex, was $1.54 \times 10^{-2}\ MW_t\ m^{-1}$ with a standard deviation of $2.1 \times 10^{-3}\ MW_t\ m^{-1}$ (Fig. 8). The minimum and maximum values were $1.08 \times 10^{-2}\ MW_t\ m^{-1}$ and $2.06 \times 10^{-2}\ MW_t\ m^{-1}$, respectively. For an approximate reservoir width of 5 km, the mean estimated geothermal potential was 77 MW_t, while the minimum and maximum values were 54 MW_t and 103 MW_t. This reservoir width corresponds to the average outcrop width of the Cajamarca Complex, as it can be observed in the geological map (Fig. 2).

The mean thermal energy for Case B, considering temperature dependent thermal conductivity in the Cajamarca Complex, was $1.88 \times 10^{-2}\ MW_t\ m^{-1}$ with a standard deviation of $2.91 \times 10^{-3}\ MW_t\ m^{-1}$. The minimum and maximum values were $1.28 \times 10^{-2}\ MW_t\ m^{-1}$ and $2.59 \times 10^{-2}\ MW_t\ m^{-1}$, respectively (Fig. 8). Considering the same reservoir width of 5 km, the mean estimated geothermal potential was now 94 MW_t, while the minimum and maximum values were 64 MW_t and 130 MW_t, respectively.

6. Discussion

This paper presented an estimation of the geothermal potential of an area of approximately 1 km^2 to the northwest of the Nevado Del Ruiz (NDR) volcano (Colombia). The work consisted in collecting rock samples in surface outcrops, measuring thermal conductivity of the rock samples with a needle probe in the laboratory, estimating heat capacity based on mesoscopic description of rock type, inferring a geological cross-section, simulating temperature at depth with numerical modeling of steady-state groundwater flow and heat transfer and conducting an uncertainty analysis using Montel Carlo simulations.

Numerical modeling based on the finite element method is recommended for the estimation of geothermal potential (Aravena et al., 2016), since it provides a rigorous way to evaluate and understand conceptual models and the system heat transfer mechanisms. Similarly, González-Garcia and Jessell (2016) stated that numerical modeling of heat and mass transfer in a hydrothermal system is a proper tool to provide a quantitative estimate of geothermal resources, as well as to aid in the sustainable management of these resources. Therefore, numerical modeling was used here as a tool helping to deal with topography and thermal conductivity distribution constrained by the inferred geology, to provide an estimation of the geothermal resources in the study area. Modeling results indicated that the Cajamarca Complex, characterized by a thermal conductivity of 2.9 $W\ m^{-1}\ K^{-1}$ can host potential basement reservoirs, as also suggested by Almaguer (2013), where the presence of secondary porosity will allow water circulation since the rock matrix has a low primary porosity. The Andesite unit, characterized by low thermal conductivity of 1.2 $W\ m^{-1}\ K^{-1}$, can provide insulation or thermal blanketing effect.

The average thermal power estimated with Monte Carlo simulations was $1.54 \times 10^{-2}\ MW_t\ m^{-1}$ (homogenous thermal conductivity) and $1.88 \times 10^{-2}\ MW_t\ m^{-1}$ (temperature dependent thermal conductivity) per meter of thickness of the potential reservoir and for an area of 1 km^2 located outside the Los Nevados NNP. This estimation is based on thermal conductivity measurements in surface samples and on the simulation of the geothermal gradient with a numerical model to anticipate temperature up to a depth of 2 km. The use of these variables and the hypothesis selected to estimate the temperature at depth can obviously affect the resources evaluation. However there is currently a lack of information about the behavior of the rock thermal conductivity at depth that could be obtained in the future from deep wells to further constrain temperature observations and calibrate the numerical model. Nevertheless, with available information in the study area facing early exploration stage, the estimated geothermal resource is thought to be representative of the current state of knowledge that will be improved as exploration proceeds to verify additional hypothesis that can influence heat transfer mechanisms at depth.

A utilization efficiency factor was used to evaluate the electrical generation potential. This factor depends on the geothermal fluid temperature (Williams et al., 2008) and is calculated by comparing the actual power output to the maximum theoretical power that could be produced from the given geothermal fluid (DiPippo, 2012).

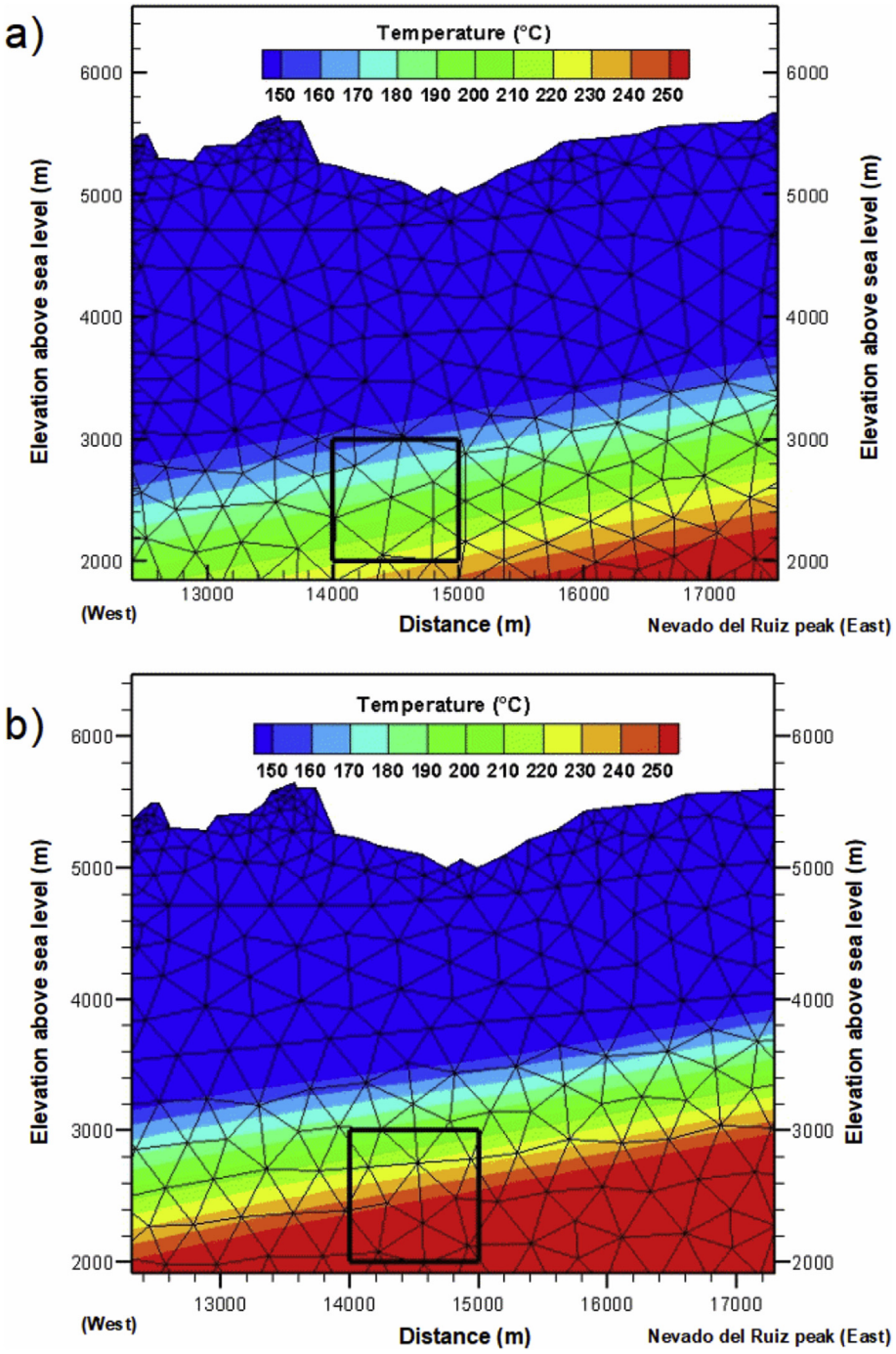

Fig. 7. Simulated temperatures and triangular mesh in the zone of interest for a) Case A and b) for Case B.

Table 5
Geothermal resource evaluation per km^2 of potential reservoir section.

Scenario	Q_R Total energy (J m^{-1}) (Eq. (4))	P_G Geothermal power (MW$_t$ m^{-1}) (Eq. (5))
Case A	5.38×10^{14}	1.36×10^{-2}
Case B	6.60×10^{14}	1.67×10^{-2}

An efficiency of 0.4 has been reported for systems of high temperature (above 150 °C; Muffler and Cataldi, 1978; Williams et al., 2008).

Further research steps shall consider the heterogeneity of the lithologic units, in other to identify and collect samples of the different type of rocks constituting the formations and estimate its thermal conductivity distribution. This additional work is important for the highly heterogeneous formations like the Quebradagrande and the Cajamarca complexes. Additional thermal conductivity measurements will further help to take into account the impact of heterogeneity in the Monte Carlo simulations and quantify its effect for the resource estimation. Only temperature at depth and recovery factor were included in this work for the uncertainty analysis. Petrophysical properties could be taken into account to help scale up thermal properties and better define their

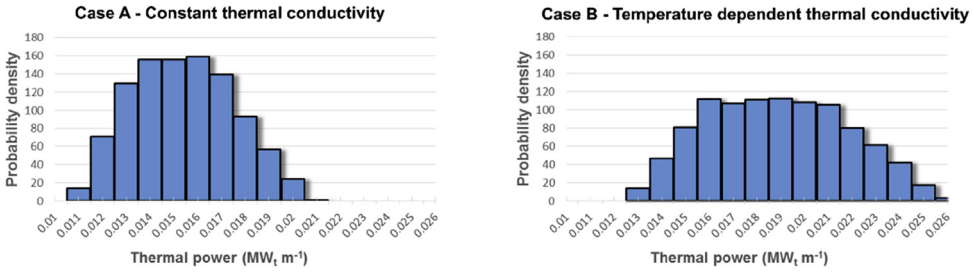

Fig. 8. Geothermal power uncertainty analysis conducted with RISK.

distribution in next research steps, when further deep well data becomes available, to finally refine Monte Carlo analysis of geothermal resources.

7. Conclusions

The thermal power estimated in this study can be compared to the electric power of 50 MW_e mentioned by Mejía et al. (2014), assuming a utilization factor of 0.4 and a reservoir width of 5 km. The electric power would consequently be comprised within the range 30–40 MW_e for the potential reservoir considering both scenarios (Case A and B), thus close to the estimation mentioned by Mejía et al. (2014). Nevertheless, the current study provides a more detailed analysis of the NDR geothermal resource potential by describing the complete methodology to obtain the final power estimates.

The uncertainty analysis allowed identifying the influence of the reservoir temperature and the recovery factor as input variables on the geothermal power estimate. A change in the reservoir temperature has a greater effect on the estimated thermal power than a change in the possible recovery factor.

An accurate measurement of the heat flow over the study area, with continuous downhole temperature profiles and thermal conductivity measurements on core samples, will help to better estimate and model the temperature at depth to reduce resource uncertainty in the future. 3D geomodeling combined with new deep exploratory wells will further improve the inferred geological cross-section to the benefit of the geothermal potential estimation. Geomodeling will be particularly useful to better characterize the geological contact between the Cajamarca Complex, potential fractured reservoirs and the Andesite unit since this contact is a key factor to evaluate the temperature at depth. Additionally, since the Cajamarca Complex is highly heterogeneous, detailed field investigations are required to improve its description. Further work will focus on the characterization of fault systems associated with hot springs and on the numerical simulation of reservoir exploitation with production and injection wells. Such logical steps are needed to move forward with the development of geothermal energy in Colombia, providing critical knowledge to support energy decisions.

This work is a valuable contribution to geothermal resource assessment that can be applied to eventually evaluate the total resource in Colombia. Geothermal resources still has to be defined at the Tufiño-Chiles-Cerro Negro geothermal system at the Colombia-Ecuador border, the Azufral, Purace, and Galeras volcanoes, and the Paipa and San Diego areas, which are the regions where exploration studies have been conducted or hydrothermal systems have been observed (Alfaro, 2015). The same methodology can be useful for other countries of South America. Several countries such as Bolivia, Argentina, Ecuador and Peru are looking for geothermal resources exploitation although no geothermal capacity was installed in this region up to 2015 (Bertani, 2016). The first geothermal power plant in South America started delivering electricity to the interconnected grid deserving northern Chile in March 2017,[2] highlighting and important step in the history of geothermal energy in South America. Geothermal resource assessment studies are required to support the development of such projects.

Acknowledgments

This work was conducted in the context of a research project funded by the Universidad de Medellín (Medellín, Colombia) in collaboration with the Institut national de la recherche scientifique (Québec, Canada). Thanks to the Canadian Department of Foreign Affairs, Trade and Development who assigned the Emerging Leaders in the Americas Program scholarships to Maria Isabel Vélez and Sebastian Cordoba in 2015. Thanks to Thomas Kalbacher for his help with the software OpenGeoSys and to two anonymous reviewers contributing to the improvement of the original paper.

The IGCP, UNESCO, and IUGS are finally acknowledged since this work is part of the project "IGCP 636-Unifying international research forces to unlock and strengthen geothermal exploitation of the Americas and Europe", currently funded by UNESCO (United Nations Educational, Scientific and Cultural Organization) and IUGS (International Union of Geological Sciences) within the International Geoscience Programme (IGCP).

References

Alfaro, C., 2015. Improvement of Perception of the Geothermal Energy as a Potential Source of Electrical Energy in Colombia, Country Update. Paper Presented at the World Geothermal Congress, p. 15. Melbourne, Australia.

Almaguer, J.L., 2013. Estudios magnetotelúrico con fines de interés geotérmico en sector Norte del Nevado del Ruíz, Colombia. MSc thesis. Universidad Nacional Autónoma de México, p. 139.

ASTM - American Society for Testing and Materials, 2008. Standard Test Method for Determination of Thermal Conductivity of Soil and Soft Rock by Thermal Needle Probe Procedure, Vol. D5334–08), p. 9.

Arango, E.E., Buitrago, A.J., Cataldi, R., Ferrara, G.C., Panichi, C., Villegas, V.J., 1970. Preliminary study on the Ruiz geothermal project (Colombia). Geothermics 2 (1), 43–56. https://doi.org/10.1016/0375-6505 (70)90005-2.

Aravena, D., Muñoz, M., Morata, D., Lahsen, A., Parada, M.Á., Dobson, P., 2016. Assessment of high enthalpy geothermal resources and promising areas of Chile. Geothermics 59, 1–13. https://doi.org/10.1016/j.geothermics.2015.09.001. Part A.

Barylo, A., 2000. Assesment of the energy potential of the Beregovsky geothermal system. In: Ukraine Geothermal Training Programme, pp. 29–42. Iceland.

Bédard, K., Comeau, F.-A., Millet, E., Raymond, J., Malo, M., Gloaguen, E., 2016. Évaluation des ressources géothermiques du bassin des Basses-Terres du Saint-Laurent. Research Report 1659. Institut national de la recherche scientifique - Centre Eau Terre Environnement, p. 100.

Bernal, N.F., Ramirez, G., Alfaro, C.V., 2000. Mapa geotérmico de Colombia. Versión 1.0. Escala 1:1'500.000. In: Memoria explicativa. Exploración y Evaluación de Recursos Geotérmicos. Instituto de investigación e información geocientífica,

[2] http://www.cega.ing.uchile.cl/en/noticias/primera-planta-geotermica-de-sudamercia-comienza-sus-operaciones-en-el-norte-de-chile/.

minero-ambiental y nuclea INGEOMINAS, p. 51.
Bertani, R., 2009. Geothermal energy: an overview on resources and potential. In: Popovski, k., Vranovska, A., Popovska Vasilevska, S. (Eds.), Proceedings of the International Conference on National Development of Geothermal Energy Use and International Course/EGEC Business Seminar on Organization of Successful Development of a Geothermal Project, p. 19.
Bertani, R., 2016. Geothermal power generation in the world 2010-2014 update report. Geothermics 60, 31–43. https://doi.org/10.1016/j.geothermics.2015.11.003.
Böttcher, N., Watanabe, N., Görke, U.-J., Kolditz, O., 2016. Geoenergy Modeling I. Geothermal Processes in Fractured Porous Media. SpringerBriefs in Energy. Computational Modeling of Energy Systems, p. 117.
Bucker, C., Rybach, L., 1996. A simple method to determine heat production from gamma-ray logs. Mar. Petroleum Geol. 13 (4), 373–375.
Calcagno, P., Baujard, C., Guillou-Frottier, L., Dagallier, A., Genter, A., 2014. Estimation of the deep geothermal potential within the Tertiary Limagne basin (French Massif Central): an integrated 3D geological and thermal approach. Geothermics 51 (0), 496–508. https://doi.org/10.1016/j.geothermics.2014.02.002.
Carslaw, H.S., Jaeger, J.C., 1947. Conduction of Heat in Solids. Oxford University Press, Oxford,UK.
CHEC - Central Hidroeléctrica de Caldas, Instituto Colombiano de Energía Eléctrica, Consultoría Técnica Colombiana Ltda, Geotérmica Italiana, 1983. Investigación Geotérmica Macizo Volcánico del Ruíz. In: Etapa, A. (Ed.), Fase II, vols. II, III. Bogotá).
Clauser, C., 2014. Thermal storage and transport properties of rocks, II: thermal conductivity and diffusivity. In: Gupta, Harsh K. (Ed.), Encyclopedia of Solid Earth Geophysics. Part of the Series Encyclopedia of Earth Sciences Series. Springer Netherlands, pp. 1431–1448.
CORPOCALDAS, 2007. Plan de manejo de los páramos del departamento de Caldas, p. 133. Technical report.
Decagon Devices Inc, 2008. KD2 Pro Thermal Properties Analyzer Operator's Manual Version 12. Decagon Devices, Inc, p. 72.
DiPippo, R., 2012. Geothermal Power Plants: Principles, Applications, Case Studies and Environmental Impact, 3 ed. Butterworth-Heinemann, Massachusetts, UE, p. 624.
Forero, J.A., 2012. Caracterización de las alteraciones hidrotermales en el flanco Noroccidental del Volcán Nevado del Ruiz, Colombia. MSc thesis. Universidad Nacional de Colombia, Bogotá, p. 121.
Freeze, A.R., Cherry, J.A., 1979. Groundwater. Prentice-Hall, p. 604.
Fridleifsson, I.B., 2003. Status of geothermal energy amongst the world's energy sources. Geothermics 32 (4–6), 379–388. https://doi.org/10.1016/j.geothermics.2003.07.004.
Geuzaine, C., Remacle, J.-F., 2009. A three-dimensional finite element mesh generator with built-in pre- and post-processing facilities. Int. J. Numer. Methods Eng. 79 (11), 1309–1331.
González-Garcia, J., Jessell, M., 2016. A 3D geological model for the Ruiz-Tolima Volcanic Massif (Colombia): assessment of geological uncertainty using a stochastic approach based on Bézier curve design. Tectonophysics 687 (26), 139–157.
González-Garcia, J., Hauser, J., Annetts, D., Franco, J., Vallejo, E., Regenauer-Lieb, K., 2015. Nevado del Ruiz volcano (Colombia): a 3D model combining geological and geophysical information. In: Proceedings World Geothermal Congress (Melbourne, Australia).
González, H., 2001. Geología de las planchas 206 Manizales y 225 Nevado del Ruíz. Memoria explicativa. Instituto de investigación e información geocientífica, minero-ambiental y nuclear, INGEOMINAS, Bogotá, p. 93.
INGEOMINAS, 2000. Mapa de flujos de calor-.
Invernizzi, C., Pierantoni, P.P., Chiodi, A., Maffucci, R., Corrado, S., Baez, W., Tassi, F., Giordano, G., Viramonte, J., 2014. Preliminary assessment of the geothermal potential of Rosario de la Frontera area (Salta, NW Argentina): insight from hydro-geological, hydro-geochemical and structural investigations. J. S. Am. Earth Sci. 54, 20–36.
Lee, K.C., 1996. Classification of geothermal resources – an engineering approach. In: Proceedings, Twenty-first Workshop on Geothermal Reservoir Engineering, Standford University, Stanford, California, January 22–24, p. 8. SGP-TR-151.
Londoño, J.M., Sudo, Y., 2002. Velocity structure and a seismic model for Nevado del Ruiz Volcano (Colombia). J. Volcanol. Geotherm. Res. 119 (1–4), 61–87. https://doi.org/10.1016/S0377-0273 (02)00306-2.
Mejía, E., Rayo, L., Méndez, J., Echeverri, J., 2014. Geothermal development in Colombia. In: Short Course VI on Utilization of Low- and Medium-enthalpy Geothermal Resources and Financial Aspects of Utilization, p. 7. Santa Tecla, El Salvador.
Mejía, E., Velandia, F., Zuluaga, C.A., López, J.A., Cramer, T., 2012. Análisis estructural al noreste del Volcán Nevado de Ruíz Colombia – aporte a la Exploración Geotérmica. Bol. Geol. 34 (1), 27–41.
Melson, W.G., Allan, J.F., Jerez, D.R., Nelen, J., Calvache, M.L., Williams, S.N., Fournelle, J., Perfit, M., 1990. Water contents, temperatures and diversity of the magmas of the catastrophic eruption of Nevado del Ruiz, Colombia. J. Volcanol. Geotherm. Res. 41 (1), 97–126. November 13, 1985. https://doi.org/10.1016/0377-0273 (90)90085-T.
Monsalve, M.L., Rodriguez, G.I., Mendez, R.A., Bernal, N.F., 1998. Geology of the well Nereidas 1, Nevado del Ruiz volcano. Colomb. Geotherm. Resour. Counc. 22, 6.
Mosquera, D., Marín, P., Vesga, C., González, H., 1998a. Geología de la Plancha 225 Nevado del Ruíz.
Mosquera, D., Marín, P., Vesga, C., González, H., Maya, M., 1998b. Geología de la Plancha 206 Manizales.
Muffler, P., Cataldi, R., 1978. Methods for regional assessment of geothermal resources. Geothermics 7 (2), 53–89. https://doi.org/10.1016/0375-6505 (78)90002-0.
Naranjo, J.L., Sigurdsson, H., Carey, S.N., Fritz, W., 1986. Eruption of the Nevado del Ruiz Volcano, Colombia, On 13 November 1985: tephra Fall and Lahars. Science 233 (4767), 961–963. https://doi.org/10.1126/science.233.4767.961.
Ofwona, C., 2008. Geothermal Resource Assessment-Case Example, Olkaria I, p. 8. Geothermal Training Programme.
Parques Nacionales Naturales de Colombia - Dirección Territorial Noroccidente, 2007. Plan de Manejo 2007-2011. Parque Nacional Natural de Los Nevados, p. 37.
Rayo-Rocha, L., Zuluaga, C.A., 2011. Procesos magmáticos en el volcán Nevado del Ruiz: un análisis cuantitativo textural. Bol. Geol. 33 (2), 59–72.
Rojas, O.E., 2012. Contribución al modelo geotérmico asociado al sistema volcánico Nevado del Ruiz-Colombia, por medio del análisis de la relación entre la susceptibilidad magnética, conductividad eléctrica y térmica del sistema. MSc thesis. Universidad Nacional de Colombia, Bogotá, p. 183.
Stefánsson, V., 1998. Estimate of the World Geothermal Potential. The United Nations University. 20th Anniversary Workshop, p. 10. Geothermal training programme, Iceland.
Stefánsson, V., 2005. World geothermal assessment. In: Proceedings World Geothermal Congress, p. 6. Amtalya, Turkey.
Stix, J., Layne, G.D., Williams, S.N., 2003. Mechanisms of degassing at Nevado del Ruiz volcano, Colombia. J. Geol. Soc. Lond. 160, 507–521.
Thouret, J.-C., 1990. Effects of the November 13, 1985 eruption on the snow pack and ice cap of Nevado del Ruiz volcano, Colombia. J. Volcanol. Geotherm. Res. 41 (1), 177–201. https://doi.org/10.1016/0377-0273 (90)90088-W.
Trenkamp, R., Kellogg, J.N., Freymueller, J.T., Mora, H.P., 2002. Wide plate margin deformation, southern Central America and northwestern South America, CASA GPS observations. J. S. Am. Earth Sci. 15 (2), 157–171. https://doi.org/10.1016/S0895-9811 (02)00018-4.
Turcotte, D.L., Schubert, G., 2014. Geodynamics. Cambridge Univerity Press, p. 657.
Vatin-Pérignon, N., Goemans, P., Oliver, R.A., Parra, E., 1990. Evaluation of magmatic processes for the products of the Nevado del Ruiz Volcano, Colombia from geochemical and petrological data. J. Volcanol. Geotherm. Res. 41 (1–4), 153–176. https://doi.org/10.1016/0377-0273 (90)90087-v.
Walsh, W., 2013. Geothermal resource assessment of the clarke lake gas field, fort nelson, british columbia. Bull. Can. Petroleum Geol. 61 (3), 241–251.
Waples, D., Waples, J., 2004. A review and evaluation of specific heat capacities of rocks, minerals, and subsurface fluids. Part 1: minerals and nonporous rocks. Nat. Resour. Res. 13 (2), 97–122. https://doi.org/10.1023/B:NARR.0000032647.41046.e7.
Westaway, R., Younger, P.L., 2013. Accounting for palaeoclimate and topography: a rigorous approach to correction of the British geothermal dataset. Geothermics 48, 31–51.
Williams, C.F., Reed, M.J., Mariner, R.H., 2008. A review of methods applied by the US Geological Survey in the assessment of identified geothermal resources. U. S. Geol. Surv. Open-File Rep. 1296 (27), 30.
Yang, F., Liu, S., Liu, J., Pang, Z., Zhou, D., 2015. Combined Monte Carlo simulation and geological modeling for geothermal resource assessment: a case study of the xiongxian geothermal field, China. In: World Geothermal Congress, p. 8. Melbourne, Australia.